Polymer 50 (2009) 3967–3973

Contents lists available at ScienceDirect

Polymer

journal homepage: www.elsevier.com/locate/polymer

Study of crystalline and amorphous phases of biodegradable poly(lactic acid) by advanced thermal analysis☆

A. Magoń [a], M. Pyda [a,b,c,*]

[a] Department of Chemistry, Rzeszów University of Technology, 35-959 Rzeszów, Poland
[b] Department of Pharmacy, Poznan University of Medical Sciences, 61-701 Poznan, Poland
[c] ATHAS-MP Company, Knoxville, TN 37922, USA

ARTICLE INFO

Article history:
Received 30 January 2009
Received in revised form
8 June 2009
Accepted 11 June 2009
Available online 27 June 2009

Keywords:
Poly(lactic acid)
Glass transition
Crystallinity

ABSTRACT

The qualitative and quantitative thermal analysis of biodegradable poly(lactic acid) PLA is presented. The glass transition, melting process, and heat capacity of a semi-crystalline poly(lactic acid) are studied utilizing the differential scanning calorimetry and temperature-modulated DSC. The mobile amorphous fraction, W_a degree of crystallinity, W_c and rigid-amorphous fraction, W_{RAF} were estimated depending on the thermal history of semi-crystalline PLA. From qualitative thermal analysis, the glass transition of rigid-amorphous phase was observed as a broadening from the changes of heat-flow-rate between mobile glass transition temperature and melting temperature. The amount of the rigid-amorphous fraction (RAF) was evaluated from $W_{RAF} = 1 - W_c - W_a$ and graphically was presented as the result of a deflection from the linearity of the dependence of the change of degree of mobile amorphous phase (W_a) vs. the degree of crystalline fraction (W_c) for semi-crystalline PLA with different thermal history. The degree of crystallinity of semi-crystalline samples of PLA can be discussed in terms of a two- or three-phase model. In contrast, the quantitative thermal analysis of the experimental apparent heat capacity of semi-crystalline PLA did not show any appearance of RAF in the examples of analyzed samples. The experimental heat capacity of PLA was analyzed in reference to the solid and liquid equilibrium heat capacities of poly(lactic acid) found in the ATHAS Data Bank.

1. Introduction

Poly(lactic acid) belongs to the aliphatic polyester group with different stereo-chemical nature L, D and *meso*-lactide with the chiral center, a carbon with the C* designation in the repeating unit:

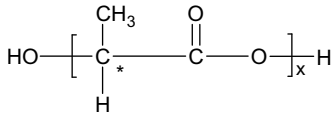

Its repeating unit has a molar mass of 72.06 g mol^{-1}. Poly(lactic acid) can be semi-crystalline or a fully amorphous material, depending on its stereo-chemical structure and thermal history.

In general, understanding all of the thermal properties of biodegradable poly(lactic acid) (PLA) requires the quantitative thermal analysis and interpretation of measured quantity, such as heat capacity, in terms of the molecular motion [1–3]. The use of proper equilibrium baselines of the 100% solid and 100% liquid heat capacities C_p is necessary to be used as references for the discussion of phase transitions. This has already been established using the Advanced THermal Analysis System (ATHAS) [2–5].

Determination of the mobile amorphous fraction, rigid-amorphous fraction and crystallinity for semi-crystalline polymeric material such as poly(lactic acid) requires also this quantitative thermal analysis. The thermal analysis of semi-crystalline poly(lactic acid) is often complicated by overlapping irreversible effects [6–15] between the glass transition and melting such as enthalpy relaxation, cold crystallization, reorganization, annealing and pre-melting processes. The kinetic effects are superimposed on the thermodynamic C_p [5–14].

In this paper, the qualitative and quantitative thermal analyses of crystallinity, the mobile amorphous fraction, and the rigid-amorphous fraction of semi-crystalline poly(lactic acid) with different thermal histories introduced by isothermal crystallization at different temperature are performed using differential scanning calorimetry

☆ Presented in part at the 3rd International Seminar on Modern Polymeric Materials For Environmental Applications, Kraków, 14–16 May 2008.

* Corresponding author. Department of Chemistry, Rzeszów University of Technology, 35-959 Rzeszów, Poland.
E-mail address: mpyda@utk.edu (M. Pyda).

0032-3861/$ – see front matter © 2009 Elsevier Ltd. All rights reserved.
doi:10.1016/j.polymer.2009.06.052

(DSC) and temperature-modulated DSC (TMDSC) to identify and describe possible contains of all these three phases in PLA.

2. Experimental part

2.1. Samples

The poly(lactic acid), PLA, was obtained from NatureWorks, LLD, USA. Poly(lactic acid) samples with a stereoisomer composition of 1.2–1.6% D-isomer lactide (PLA-4032D), and a weight-average molecular weight of 220 kDa, were used in standard DSC and temperature-modulated DSC studies.

In order to obtain semi-crystalline PLA, the samples were placed inside of the DSC cell and were cooled at a rate of about $q = 50\ \mathrm{K\,min^{-1}}$ from the melt to given crystallization temperatures (T_c) where sample was crystallized isothermally for given time, then the cool continued at a rate around $50\ \mathrm{K\,min^{-1}}$ to below mobile glass transition and finally reheating with rate mostly of $10\ \mathrm{K\,min^{-1}}$. It should be noted that not all cooling processes inside of DSC were well controlled. Fig. 1 shows an example of experimental thermogram of heat-flow-rate at various temperatures of PLA-4032D on cooling, heating and also including isothermal crystallization by standard DSC. The inserted picture in Fig. 1 shows the programmed temperature during all traces for result presented in Fig. 1.

Single-crystalline sapphire (Al_2O_3) was used to calibrate the heat capacity at each temperature. The temperature calibration was performed with the extrapolated onset temperatures of the phase transitions of indium $T_m = 429.75\ \mathrm{K}$ (156.6 °C).

For measurements by standard DSC, samples of 10–15 mg were used, for temperature-modulated calorimetry the sample weights were 4–10 mg, weighed on a Cahn C-28 electrobalance to an accuracy of (0.001 mg). The samples for DSC and TMDSC were analyzed in aluminum pans of about 24 mg and heat-treated in these aluminum pans in the calorimeter.

2.2. Measurement and instrumentation

All measurements were performed on the heat-flux differential scanning calorimeter DSC, Q1000™ from TA Instruments, Inc., equipped with a mechanical refrigerator from temperatures 183.15 K (−90 °C) to 483.15 K (210 °C). Dry nitrogen gas with a flow rate of $50\ \mathrm{mL\,min^{-1}}$ was purged through the DSC cell in the instrument. DSC, Q1000™ was used to obtain the heat-flow rates, transition parameters, apparent total and reversing heat capacities. Cooling was accomplished with a refrigerated cooling system.

The experiments were performed in two modes:

2.2.1. Standard DSC

Measurements were performed on heating: a) after isothermal crystallization with different temperature T_c and time (from 300 to 900 min) of crystallization when the samples were cooled at rate of about $q = 50\ \mathrm{K\,min^{-1}}$, to below the glass transition and reheated at a heating rate of $10\ \mathrm{K\,min^{-1}}$, b) after non-isothermal crystallization on cooling rate, from 30 to $0.5\ \mathrm{K\,min^{-1}}$ from melt to the region below T_g to obtain different degrees of crystallinity.

For the quantitative DSC measurements, three runs were carried out: one with an empty reference and a sample pan, to correct for asymmetry of the DSC, one with an empty reference pan and a pan filled with sapphire for calibration, and one with an empty pan and a pan filled with the sample. After the steady state was obtained, the C_p was determined using the following equation:

$$C_p = K \cdot \frac{\Delta T}{q} + C_S \cdot \frac{d\Delta T}{dT_s} \quad (1)$$

where K is determined as a function of temperature from the sapphire calibration, ΔT is the temperature difference between reference and sample, proportional to the heat-flow rate, HF; C_s is the heat capacity of the sample calorimeter including sample and aluminum pan, and T_s is the sample temperature. The resulting C_s was internally calibrated using the baselines from the ATHAS Data Bank for the solid and liquid.

2.2.2. Quasi-isothermal TMDSC

Quasi-isothermal temperature-modulated DSC (TMDSC) [2] measurements were performed around the constant temperature $T_c = 373{,}15\ \mathrm{K}$, (100 °C) with the modulation amplitude of 0.5 K and period of 60 s, after cooling the sample at around constant rate of $q = 50\ \mathrm{K\,min^{-1}}$, from the melt to crystallization temperature, T_c and isothermal crystallization at this temperature T_c.

For quasi-isothermal TMDSC measurement, the underlying heating rate was equal to zero, $\langle q \rangle = 0$ and the range of temperature of interest was covered by run at T_c. The results consist only of the apparent reversing C_p, expressed by:

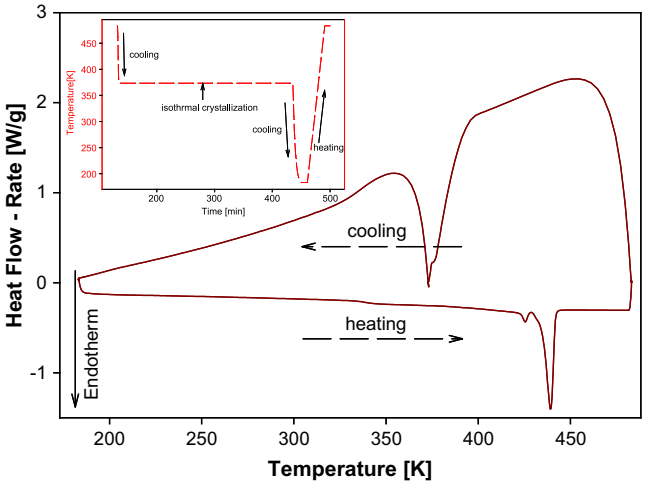

Fig. 1. An example of experimental data of heat flow rate vs. temperature on cooling and heating by standard DSC. The inserted picture shows the programmed temperature for presented result.

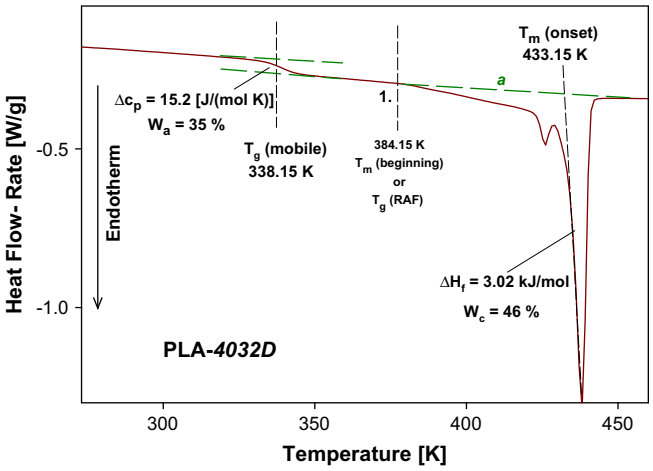

Fig. 2. Experimental DSC curve as heat-flow rate plotted against temperature on heating at $10\ \mathrm{K\,min^{-1}}$ of semi-crystalline poly(lactic acid), PLA-4032D. The sample was kept isothermally at $T = 373.15\ \mathrm{K}$ (100 °C) for 5 h on the cooling from the melt.

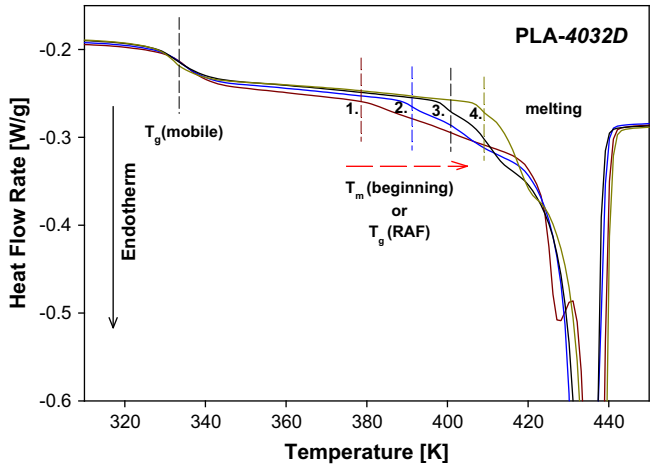

Fig. 3. Heat-flow rate vs. temperature of poly (lactic acid), PLA-4032D with different thermal histories by standard DSC on heating at 10 K min^{-1}: after isothermal crystallization at $T_c = 373.15$ K for 5 h, (curve 1.) as was shown in Fig. 1, after isothermal crystallization at $T_c = 383.15$ K for 5 h, (curve 2.) at $T_c = 393.15$ K for 5 h(curve 3.) and at $T_c = 403.15$ K for 5 h (curve 4.).

$$C_p(\text{reversing}) = \sqrt{C_{\text{real}}^2 + C_{\text{im}}^2} = \frac{\langle A_\Phi \rangle}{\langle A_{T_s} \rangle \omega} \cdot K(\omega); \quad (2)$$

where C_p(reversing) is the modulus of the complex heat capacity, ($C_p = C_{\text{real}} + iC_{\text{im}}$) with its real, C_{real}, and imaginary, C_{im}, parts, respectively; $\langle A_\Phi \rangle$ is the heat-flow rate amplitude, smoothed over one modulation cycle;$\langle A_{T_s} \rangle$ is the similarly smoothed modulation amplitude of T_s; and $K(\omega) = \sqrt{1 + \tau^2\omega^2}$ is Newton's law constant and $K(\omega)$ is a frequency-dependent calibration factor with τ being a correction used when analyzing the C_p at a different frequency then the calibration. Under the usual conditions of continued linearity and stationary, τ is a constant ($=C_r/K$), where C_r is the C_p of the empty reference pan and K is the constant, as before.

The evaluation of data from standard DSC and temperature-modulated TMDSC was carried out by using TA Instrument and Math 3.0 software. The C_p(reversing) was obtained from a Fourier deconvolution of the first harmonic of the modulated quantities using the TA Instrument software.

3. Results

Figs. 1–3 display a series of the experimental heat-flow rates vs. temperature of poly(lactic acid), PLA-4032D with different thermal histories by standard DSC on heating at 10 K min^{-1} after isothermal crystallization at different temperatures ranging from 373.15 K (100 °C) to 403.15 K (130 °C) for 5 h respectively.

Fig. 2 shows the heat-flow rate vs. temperature on heating at 10 K min^{-1} (low portion of results presented on Fig. 1) of PLA-4032D sample after isothermal crystallization at 373.15 K (100 °C) for 5 h and its qualitative thermal analysis. Changes of heat-flow rate around the temperature of 338.15 K (65 °C), T_g(mobile) are related with a mobile glass transition. Change of heat capacity at T_g(mobile) from qualitative analysis between two asymptotic lines was estimated as $\Delta C_p = 15.20$ J/(mol^{-1} K^{-1})] which gives $W_a = 35\%$ mobile amorphous fraction (MAF) in the examined semi-crystalline sample. Changes of heat-flow rate occur in Fig. 2 during heating in higher temperature, around 384.15 K (111 °C) can be related with the beginning of melting process T_m(beginning) of crystal or with an devitrification of the mesophase, rigid-amorphous fraction T_g(RAF) in the semi-crystalline PLA-4032D. Next, a completed melting process is presented as double endothermic peak with an onset of bigger melting transition temperature at 433.15 K (160 °C). The small peak in the low temperature represents a melting of non-perfect small crystal. The qualitative analysis of melting peaks for the integration using of straight baseline (curve *a*) gives a value of heat of fusion (ΔH_f) around 3.02 kJ mol^{-1} (also included in Table 1) which is related with $W_c = 35\%$ of crystalline fraction in sample.

Next, Fig. 3 presents results of the heat-flow rates of PLA after isothermal crystallization for 5 h at different temperatures such as at 373.15 K (100 °C) (curve 1.), at 383.15 K (110 °C), (curve 2.) at 393.15 K (120 °C), (curve 3.) and at 403.15 K (130 °C) (curve 4.), respectively.

Results of the whole series of measurements show the similarity of T_g(mobile) and changes of heat capacity at mobile glass transition temperature for all different crystallization temperatures. Differences in the changes of heat-flow rate in Fig. 3 appear at the beginning of melting process T_m(beginning) or may be due to the relaxation of rigid-amorphous fraction, T_g(RAF) for different isothermal crystallization temperature T_c. For higher T_c, the second step in the changes of heat-flow rates of series samples, at the T_m(beginning) or T_g(RAF) and melting peak are shifted to the higher temperature. Also the heat of fusion for higher T_c is larger. It should be noted that only curve 1. shows clear double peaks in the melting process. All characteristic parameters of results and conditions from the standard DSC evaluation shown in Fig. 3 are also presented in Table 1.

Next, heat-flow rates were converted to heat capacities and calibrated. In Fig. 4, an example of the changes of the apparent C_p of PLA-4032D with temperature is presented, as obtained from standard DSC on heating at 10 K min^{-1} after cooling from the melt and crystallized isothermally at temperature $T_c = 373.15$ K for 5 h. The experimental heat capacity of PLA-4032D was analyzed in reference to the solid, C_p(vibrational) and liquid, C_p(liquid) heat capacities of poly(lactic acid) found in the paper [3]. First, using thermal analysis, the mobile amorphous fraction, W_a was estimated from:

$$W_a = \frac{\Delta C_p}{\Delta C_p(100\%)} \quad (3)$$

where ΔC_p and ΔC_p(100%) are changes of heat capacity at T_g(mobile) of semi-crystalline and full amorphous PLA-4032D, respectively. For calculation, the value of ΔC_p (100%) used was 43.8 J K^{-1} mol^{-1} according to Ref. [3]. For the quantitative analysis of heat capacities shown in Fig. 4, equation (3) was used in the evaluation of the mobile amorphous fraction and has the following expression:

Table 1
Thermodynamics parameters and results from a qualitative evaluation of data of PLA-4032D as presented in Fig. 3.

Sample	T_c [K]	t [min][a]	T_g [K] (mobile)	ΔC_p [J/(molK)]	W_a	T_m [K] (onset)	ΔH_f [kJ/mol]	W_c	W_{RAF}
1	373.15	300	338.15	15.20	0.35	433.15	3.020	0.46	0.19
2	383.15	300	336.37	16.96	0.39	431.40	3.124	0.48	0.13
3	393.15	300	335.41	16.05	0.37	433.75	3.318	0.51	0.12
4	403.15	300	334.54	15.39	0.35	434.91	3.402	0.52	0.12

[a] t, time of crystallization.

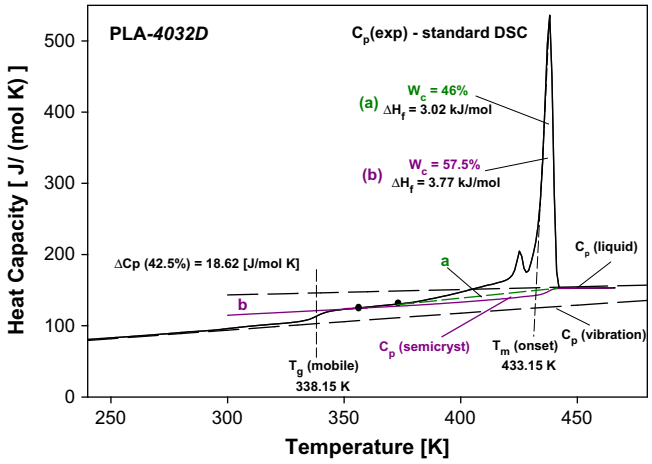

Fig. 4. Experimental heat capacity of semi-crystalline poly(lactic acid), PLA-4032D after isothermal crystallization at $T_c = 373.15$ K (100 °C) for 5 h and calculated heat capacities of solid and liquid PLA plotted against temperature from Ref. [3].

$$W_a = \frac{\Delta C_p}{\Delta C_p(100\%)} = \frac{C_p(\text{exp}) - C_p(\text{vibration})}{C_p(\text{liquid}) - C_p(\text{vibration})} \quad (3a)$$

which gives 42.5% of MAF in contrast to the result of 35% from qualitative analysis (see Fig. 2).

The degree of crystallinity, W_c was estimated from two approximations: from the so-called *zero-approximation* and *advanced-approximation*. First, the degree of crystallinity was calculated from the ratio of heat of fusion of semi-crystalline, ΔH_f (Table 1) and completed crystal, ΔH_f (100%):

$$W_c = \frac{\Delta H_f}{\Delta H_f(100\%)} \quad (4)$$

For the calculation, 6554 J mol^{-1} was used as the value of ΔH_f (100%) according to Ref. [3]. As is presented in Fig. 1, a straight line (curve *a*) was used for the integration of the area of the peak for the *zero-approximation* of ΔH_f.

The rigid-amorphous fraction, W_{RAF} was estimated as a remaining portion from the relation:

$$W_{RAF} = 1 - W_a - W_c. \quad (5)$$

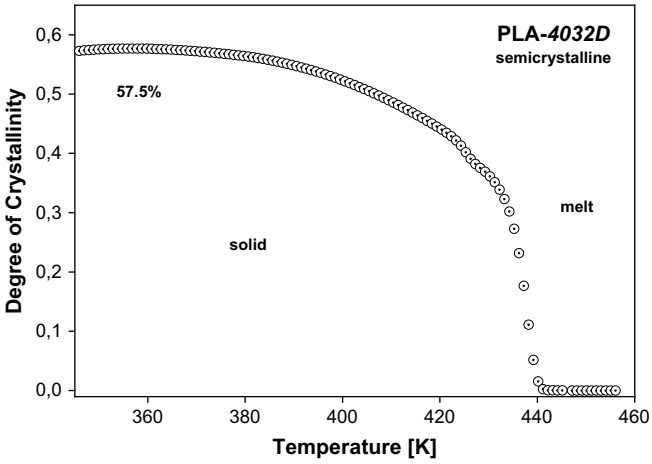

Fig. 5. Fraction of degree of crystallinity vs. temperature for semi-crystalline poly(lactic acid), PLA-4032D on the heating after isothermal crystallization at $T_c = 373.15$ K (100 °C) for 5 h.

The result of the qualitative analyses of PLA-4032D presented in Fig. 2 shows that a degree of mobile amorphous phase is $W_a = 35\%$, degree of crystallinity is $W_c = 46\%$, and the rigid-amorphous phase W_{RAF} is with a fraction of 19%.

Next, in order to continue the quantitative thermal analysis of PLA-4032D presented in Fig. 4, the degree of crystallinity was estimated by the *advanced* approach. Using the two-phase model, and assuming that semi-crystalline PLA-4032D has amorphous and crystal phases, the crystallinity as the function of temperature $W_c = f(T)$ was found from the following equation [1–3]:

$$C_p(\text{exp}) = W_c C_p(\text{solid}) + (1 - W_c) C_p(\text{liquid}) - \frac{dW_c}{dT} \Delta H_f(T) \quad (6)$$

where C_p (exp) is the experimental, apparent heat capacity, C_p (solid) and C_p (liquid) are the equilibrium heat capacity of crystal and liquid, respectively from Ref. [3]. The heat of fusion, ΔH_f (T), is represented by the temperature dependence difference enthalpy of melt and crystal, H(melt) – H(crystal). Fig. 5 presents the results of this calculation of $W_c = f(T)$ with a maximum degree of crystallinity of 57.5%.

Next, this crystallinity as a function of temperature, $W_c = f(T)$, was utilized for the calculation of expected, semi-crystalline heat capacity baseline, C_p(semicryst) from:

$$C_p(\text{semicryst}) = W_c(T) C_p(\text{solid}) + (1 - W_c(T)) C_p(\text{liquid}) \quad (7)$$

to serve for the next step of the analysis. With all of the above assumptions, the baseline C_p(semicryst) is separated from the thermodynamic heat capacity and latent heat in the apparent C_p(exp) in the melting transition region. The semi-crystalline baseline, C_p(semicryst) was shown in Fig. 4 as curve *b*. With help of this C_p(semicryst) the heat of fusion was calculated as 3.77 kJ mol^{-1} which corresponds to 57.5% of the maximum degree of crystallinity, the mobile amorphous fraction W_a is 42.5% for this case of quantitative analysis. Finally the absence of any the rigid-amorphous fraction was noted. The difference between the two crystalline fractions resulting from the two different integration baselines *b* and *a* gives a value of 11.5%. This can be a subject for discussion of improvement of our analysis of PLA.

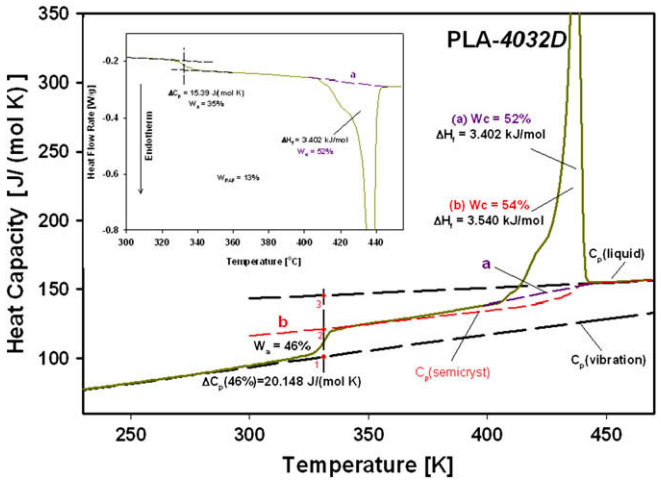

Fig. 6. Experimental heat capacity of semi-crystalline poly(lactic acid), PLA-4032D after isothermal crystallization at $T_c = 403.15$ K (130 °C) for 5 h and calculated heat capacities of solid and liquid PLA plotted against temperature from Ref. [3]. In insert picture: raw data of heat-flow rate with results from qualitative analysis of all fractions ($W_a = 0.35$, $W_c = 0.52$ and $W_{RAF} = 0.13$).

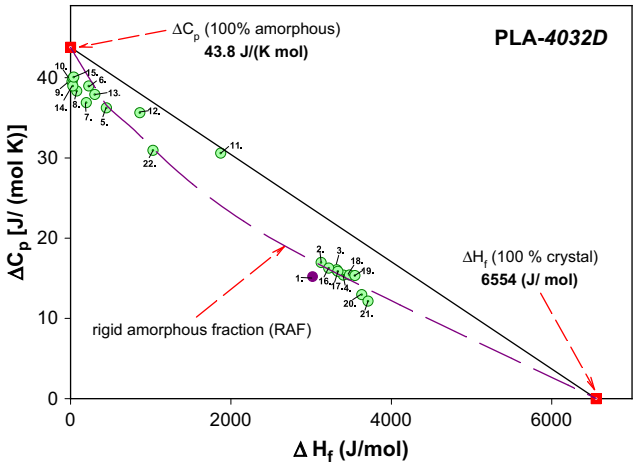

Fig. 7. Plot of changes of heat capacity at glass mobile transition temperature vs. heat of fusion of semi-crystalline poly (lactic acid), PLA-4032D with different thermal history (marked numbers correspond to samples numbered in Tables 1 and 2).

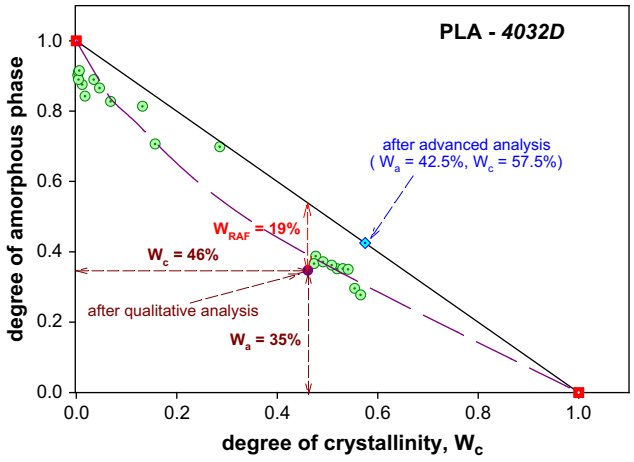

Fig. 8. Plot of degree of amorphous vs. degree of crystalline of semi-crystalline poly (lactic acid), PLA-4032D with different thermal history.

Fig. 6 with its inserted picture in the corner presents the second example of compared results from the qualitative and quantitative thermal analysis of semi-crystalline poly(lactic acid), PLA-4032D after isothermal crystallization at $T_c = 403.15$ K (130 °C) for 5 h (case 4. in Fig. 2 and in Table 1). The qualitative analysis of this sample from heat-flow rate as is presented in the small picture in Fig. 6 shows 35% of mobile amorphous fraction, 52% of degree crystallinity and 13% of rigid-amorphous fraction. In contrast, the quantitative thermal analysis of heat capacities of this PLA-4032D sample as is presented in the main part of Fig. 6 shows much more mobile amorphous fraction of 46%, also higher $W_c = 54\%$ and the absence of the rigid-amorphous fraction similar to sample 1. (see Fig. 4). The MAF was calculated for the change of C_p between point 1 and 2 in mobile glass transition temperature and heat of fusion, $\Delta H_f = 3.54$ kJ mol^{-1} was obtained from integration of the melting peak using C_p(semicryst) baseline *b*.

The changes of heat capacity, ΔC_p at the mobile glass transition temperature, T_g,(mobile) and the measured heats of fusion, ΔH_f for all samples of PLA-4032D with different thermal histories are plotted in Fig. 7. The circle points in Fig. 7 are the data from the qualitative analysis as is also reported in Figs. 2,3 and 6 and in Tables 1 and 2. The solid straight line is drawn between full amorphous and full crystalline sample of PLA represented by square points in Fig. 7. The experimental data points (circle points) show the deviation from linearity of ΔC_p vs. ΔH_f. This occurs for almost all samples. This may suggest the presence of some rigid-amorphous fraction in all PLA-4032D samples that were examined.

The data in Fig. 7 were converted to represent differently the degree of amorphous phase (eq. (1)) and degree of crystallinity (eq. (2)) and are illustrated in Fig. 8. Additional data, represented by dark circle (qualitative analysis) and diamond (quantitative analysis) points in Fig. 8, are also plotted as results of thermal analysis of semi-crystalline poly(lactic acid), PLA-4032D (see Figs. 4,6 and 10).

The most promising region for evaluation of rigid-amorphous fraction was expected on the thermal treatment during the isothermal crystallization at $T_c = 373.15$ K and later on additional cooling/heating or annealing. In order to directly observe the formation of phases during the isothermal crystallization, the quasi-isothermal method of temperature-modulated DSC (TMDSC) was applied.

The evolution of reversing heat capacity, C_p(reversing) in time-domain during isothermal crystallization of PLA-4032D at $T_c = 373.15$ K was shown in Fig. 9. The reversing heat capacity was measured by quasi-isothermal TMDSC mode with temperature

Table 2
Experimental parameters and results from evaluation of data of PLA-4032D as presented in Figs. 7 and 8.

Sample	Heating rate [K/min]	Cooling rate [K/min]	T_c [K]	t [min]	ΔC_p [J/mol K]	ΔH_f [J/mol]
5	1.0	30.0	–	–	36.24	447.49
6	2.0	30.0	–	–	38.96	228.07
7	3.0	30.0	–	–	36.90	197.01
8	5.0	30.0	–	–	38.34	77.61
9	8.0	30.0	–	–	39.50	19.59
10	10.0	30.0	–	–	39.91	28.64
11	10.0	0.5	–	–	30.60	1872.83
12	10.0	1.0	–	–	35.63	864.72
13	10.0	2.0	–	–	37.90	302.94
14	10.0	5.0	–	–	38.96	29.11
15	10.0	10.0	–	–	40.07	39.96
16	–	–	100	600	16.26	3218.92
17	–	–	100	900	15.85	3332.05
18	–	–	110	600	15.41	3477.62
19	–	–	110	900	15.33	3546.07
20	–	–	120	600	12.96	3631.10
21	–	–	120	900	12.14	3708.93
22	–	–	140	300	30.94	1028.30

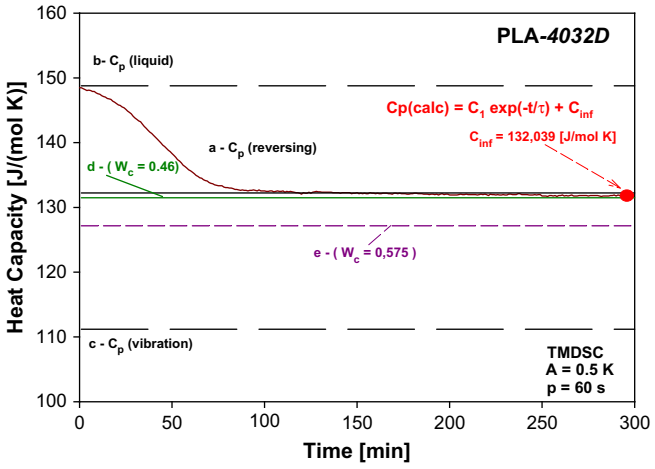

Fig. 9. Time evolution of experimental heat capacity (a) of semi-crystalline poly(lactic acid), PLA-4032D during isothermal crystallization at $T_c = 373.15$ K (100 °C) for 5 h. Curves *b* and *c* indicate the heat capacity of 100% amorphous PLA, C_p (liquid) and the vibration heat capacity of solid PLA, C_p(vibration), respectively.

amplitude $A = 0.5$ K and period $p = 60$ s around 373.15 K and the results were presented in the frame of two baselines of the vibration and liquid capacities. After approximately 300 min, the C_p (reversing) of PLA-4032D from the level of liquid state has reached the level of solid state of 132 J (mol^{-1} K^{-1}). Curves *d* and *e* of heat capacity were estimated from the qualitative and quantitative thermal analysis of three- and two-phase model with a crystallinity fraction of $W_c = 0.46$ and $W_c = 0.575$, respectively. The reached level of heat capacity provides information about the crystalline fraction forming during the isothermal crystallization.

Results in Fig. 9 show the experimental evidence that PLA-4032D is a semi-crystalline polymer. During the isothermal crystallization, which occurs at 373.15 K, only 46% of crystal phase was created. The same value of crystallinity ($W_c = 0.46$) was obtained from qualitative analysis of the heat-flow rate on heating (see Fig. 2). It means that non-additional crystalline phase was formed in the sample during cooling and reheating according to qualitative analysis. The amount of others phases: degree of mobile amorphous phase (35%) and the rigid-amorphous fraction (19%) were also obtained from this qualitative analysis as was presented earlier. In contrast, according to quantitative analysis additional crystalline phase should be formed in PLA sample 1. later on cooling or reheating to reach crystalline of 57.5%.

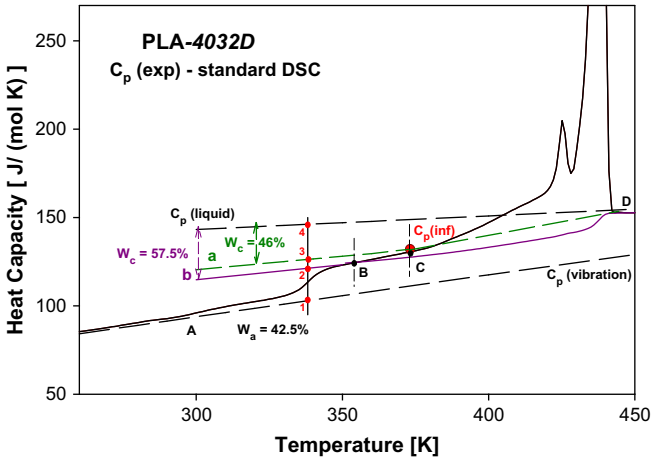

Fig. 10. Experimental heat capacity of semi-crystalline poly(lactic acid), PLA-4032D after isothermal crystallization at $T_c = 373.15$ K (100 °C) for 5 h as in Fig. 4 and the evaluation of results of phase fractions from quantitative thermal analysis.

4. Discussion

The qualitative thermal analysis of biodegradable poly(lactic acid) PLA-4032D was presented here based on the raw data of heat-flow rates and the quantitative thermal analysis based on the heat capacity. Analysis of the heat-flow rates in Figs. 2,3, and 6 suggests that PLA-4032D could be a three phase polymer, including an amorphous, crystalline and rigid-amorphous phase. For samples after isothermal crystallization at temperature between 373.15 K (100 °C) and 403.15 K (130 °C) (see Fig. 2) the changes of the ΔC_p at T_g(mobile) are similar, much significant the changes of heat-flow rates at T_m(beginning) or T_g(RAF) and at melting peak regions are observed. Since ΔC_p at T_g (mobile) are similar and the heat of fusion, ΔH_f are different, the amount of interface, rigid-amorphous fraction must be a part of the semi-crystalline PLA. The RAF of semi-crystalline samples of PLA obtained from this qualitative analysis presented in Figs. 2 and 6 were 0.19 and 0.13, respectively (see Table 1 for samples 1. and 4.). In contrast, the quantitative analysis of the same samples did not show any existing rigid-amorphous phase. The examples of the quantitative analysis for PLA-4032D were presented in Figs. 4,6 and 10. For this analysis the results of MAF show much higher values of 0.425 and 0.46 instead of the 0.35 value for both cases in qualitative thermal analysis. Also, the values of crystallinity were higher, measuring 0.575 and 0.54 instead 0.46 and 0.52, respectively. Details of the quantitative analysis PLA after crystallization at $T_c = 373.15$ K for 5 h (for sample 1. in Table 1) is shown in Fig. 10. Good agreement is observed between experimental C_p and calculated C_p (vibration), for values below T_g of 338.15 K and above melting peak T_m of 433.15 K (160 °C) for liquid heat capacity, C_p(liquid). The changes of heat capacity between point 1 and 2 at T_g are related with the devitrification of 42.5% of mobile amorphous phase from solid state (A) to high viscoelastic state (B). Next, changes of C_p(exp) between area B and D (liquid state) show the process of melting of crystal phase according as provided by employing equation (6) for two-phase models. Using the C_p (semicryst) baseline (*b* in Fig. 10) for calculation, the value of the degree of crystallinity was $W_c = 0.575$. In this case, the melting process started at point B, which is very close to the end of glass transition. No RAF was estimated from this quantitative thermal analysis for presented semi-crystalline poly(lactic acid), PLA-4032D. This result was also illustrated as a diamond point in Fig. 8. The degree of crystallinity estimated from qualitative analysis using a straight line between C and D (baseline *a* in Figs. 10,4, and 2) has reached the value of only 46%. It is interesting to note that the reversing heat capacity reached the same value of C_p(inf) of 46% during isothermal crystallization of the sample at infinite time (see point C in Fig. 8). This result suggests that the RAF can most likely form later during the process of cooling to lower temperatures or reheating instead of by isothermal crystallization. The MAF was the same as previously reported, 35% (see Fig. 2) and the rigid-amorphous fraction (RAF) was estimated as the remaining part of $W_{RAF} = 0.19 = 1 - W_c - W_a$.

No RAF was estimated from quantitative thermal analysis for the second example of semi-crystalline poly(lactic acid), PLA-4032D as was presented in Fig. 6. The same difference in the estimation of heat of fusion resulting from difference of baselines of C_p(semi-cryst) (*a* and *b* in Fig. 6) which separated heat capacity from a latent heat in the melting region was observed. As for sample 1. (see Fig. 10), all possible portions of the rigid-amorphous fraction were included in the mobile or crystal fractions for sample 4. as well (see Fig. 6).

5. Conclusion

The standard DSC, temperature-modulated DSC, and thermal analysis enable the estimation of the three phases: mobile amorphous, crystalline and rigid-amorphous phase of biodegradable poly(lactic acid) PLA. The question raised is how to estimate of fraction phases from calorimetry and thermal analysis. Both, the qualitative and quantitative thermal analysis of semi-crystalline poly(lactic acid), PLA-4032D was presented and the approaches compared. The qualitative thermal analysis of PLA-4032D based on the evaluation of the heat-flow rates has revealed the formation of three phases: mobile amorphous fraction, W_a degree of crystallinity, W_c and rigid-amorphous fraction, W_{RAF} with different thermal history. The glass transition of rigid-amorphous phase can be interpreted as broadening from changes of the heat-flow rate between mobile glass transition temperature and melting temperature or an increase at the beginning of melting process. The quantitative thermal analysis of the experimental apparent heat capacity of semi-crystalline PLA did not show any appearance of RAF in the examples of the presented samples. This result was supported partially by the experimental evidence of direct measurement of reversing heat capacity from quasi-isothermal TMDSC during isothermal crystallization. Further crystallization or formation of RAF was possible on cooling and heating. The degree of crystallinity of semi-crystalline samples of PLA can be discussed in terms of a two- or three-phase model. Quantitative analysis of results from DSC and TMDSC shows contributions of two major phases: mobile amorphous fraction and crystalline phase. In all cases observed, the intermediate phase can be included in the crystalline or the mobile amorphous phases. Special techniques of quasi-isothermal TMDSC with frequency- and amplitude-variation should be applied to obtain additional information regarding distribution of phases in examined PLA-4032D.

Acknowledgments

This work was supported by European Union Grant (MIRG-CT-2006036558) and by NatureWorks, LLD, (Cargill Dow LLD), Chem. Co. USA.

References

[1] Magon A, Pyda M. In: Proc. 3rd international seminar on modern polymeric materials for environmental application, vol. 3, Kraków; 14–16 May 2008. p. 125–30.
[2] Wunderlich B. Thermal analysis of polymeric materials. Berlin: Springer-Verlag; 2005.
[3] Pyda M, Bopp RC, Wunderlich B. J Chem Thermodyn 2004;36:731.
[4] Pyda M, Wunderlich B. Macromolecules 2005;38:10472.
[5] Pyda M. The ATHAS data bank, http://athas.prz.rzeszow.pl; 2007.
[6] Wunderlich B. Prog Polym Sci 2003;28:383.
[7] Baratian S, Hall ES, Lin JS, Xu R, Runt J. Macromolecules 2001;34:4857.
[8] Witzke DR. Introduction to properties engineering and prospects of polylactide polymers, UMI, dissertation, Michigan State University, East Lansing, MI; 1997.
[9] Schick C. Temperature modulated differential scanning calorimetry (tmdsc) – basics and applications to polymers. In: Cheng SZD, editor. Handbook of thermal analysis and calorimetry. Applications to polymers and plastics, vol. 3. Amsterdam: Elsevier Science; 2002.
[10] Schick C, Wurm A, Mohamed A. Colloid Polym Sci 2001;279:800.
[11] Penning JP, Dijkstra H, Pennings AJ. Polymer 1993;34:942.
[12] Sarasua JR, Prud'homme RE, Wisniewski M, Le Borgne A, Spassky N. Macromolecules 1998;31:3895.
[13] Cohn D, Hotovely-Salomon A. Polymer 2005;46:2068.
[14] McKenna GB, Simon SL. The glass transition: its measurements and underlying physics. In: Cheng SZD, editor. Handbook of thermal analysis and calorimetry. Applications to polymers and plastics, vol. 3. Amsterdam: Elsevier Science; 2002.
[15] Sanchez MS, Mathot VBF, Poel GV, Ribelles JLG. Macromolecules 2007;40:7989.